JOURNAL OF GEOPHYSICAL RESEARCH, VOL. 114, C00A06, doi:10.1029/2008JC005127, 2009

Atmospheric forcing of the Beaufort Sea ice gyre: Surface pressure climatology and sea ice motion

Matthew G. Asplin,[1] Jennifer V. Lukovich,[1] and David G. Barber[1]

Received 18 September 2008; revised 20 December 2008; accepted 10 February 2009; published 9 April 2009.

[1] The Beaufort Gyre (BG) typically rotates anticyclonically and exerts an important control on Arctic Sea ice dynamics. Previous studies have shown reversals in the BG to rotate cyclonically during summer months and, in recent decades, throughout the annual cycle. In this investigation, we explore the synoptic climatology of atmospheric forcing and its relationship to sea ice motion and BG reversals. A catalog of daily synoptic weather types is generated for the Beaufort Sea Region covering the period 1979 to 2006 using NCEP/NCAR reanalysis mean sea level pressure data, principle components, and k-means cluster analyses. Mean synoptic type frequency, persistence, and duration values are calculated for each synoptic type and contrasted between the summer and winter seasons. Daily synoptic types are linked to changes in sea ice vorticity by using correlation analysis on lagged sea ice vorticity data. Lag correlations are found between synoptic types and sea ice vorticity smoothed over a 12-week running mean and show that cyclonic types, which promote southerly or easterly atmospheric circulation over the southern Beaufort Sea, commonly precede summer reversals. Furthermore, significant seasonal within-type variability in sea ice vorticity is detected within the synoptic types illustrating the importance of seasonal variability on these processes.

Citation: Asplin, M. G., J. V. Lukovich, and D. G. Barber (2009), Atmospheric forcing of the Beaufort Sea ice gyre: Surface pressure climatology and sea ice motion, *J. Geophys. Res.*, *114*, C00A06, doi:10.1029/2008JC005127.

1. Introduction

[2] The Beaufort Gyre (BG) is a large ocean circulation feature that plays a significant role in regulating variability in the Arctic climate [*McLaren et al.*, 1987; *Serreze et al.*, 1989; *LeDrew et al.*, 1991; *Proshutinsky and Johnson*, 1997]. The circulation of the BG is strongly driven by synoptic-scale atmospheric circulation patterns. The prevailing atmospheric circulation pattern is anticyclonic, thus the usual rotational direction for the BG is anticyclonic (clockwise). This promotes sea ice convergence, higher ice concentrations, and increased ice ridging via Ekman convergence [*Proshutinsky et al.*, 2002]. During the summer, the BG can occasionally reverse to a cyclonic (counterclockwise) circulation pattern. Reversals of the BG are attributed to lower sea level pressure (SLP) throughout the Arctic basin, and persistent low-pressure systems occurring over the southern Beaufort Sea [*McLaren et al.*, 1987; *Serreze et al.*, 1989; *LeDrew et al.*, 1991]. *Lukovich and Barber* [2006] also identify a time-lagged response between stratospheric and upper level tropospheric relative vorticity and reversals of the BG.

[3] The influence that the BG has upon sea ice motion and sea ice concentration depends on sea ice extent, circulation regime of the gyre, and the vorticity within the gyre itself [*Barry and Maslanik*, 1989; *Lukovich and Barber*, 2006]. Sea ice velocity and vorticity values in the gyre are generally the weakest during April, when Arctic sea ice is at its maximum extent and highest concentrations, and the greatest during the summer (August and September) when ice extent and concentrations are at their annual minimum. A predominantly anticyclonic BG tends to transport sea ice away from the Canadian Archipelago, and westward into the Chukchi Sea [*Kwok*, 2006; *Lukovich and Barber*, 2006]. The amount of sea ice being exported southward through Fram Strait has also been linked to the rotational regime of the BG. During the reversals of the BG, northerly transport of sea ice from the Chukchi and southern Beaufort seas increases sea ice concentrations within the transpolar drift, hence increasing the volume of ice that is exported through Fram Strait [*Yu et al.*, 2004; *Lukovich and Barber*, 2006].

[4] Sea ice dynamics in the Arctic can also be impacted by storms (cyclones). An area of reduced ice concentration in the Canada basin in August 1981 was linked to westerly winds associated with a persistent cyclone situated to the NE [*Barry and Maslanik*, 1989]. Furthermore, a cyclone can fracture the underlying sea ice and create conditions favorable for local-scale ice divergence during and immediately following the passage of the cyclone [*Brümmer et al.*, 2003]. This may introduce coupling between the ocean-sea ice-atmosphere system where increased upward energy and moisture fluxes from the ocean may lead to the intensification of cyclones. This process would be most prevalent during the autumn and early winter seasons when there is a rapidly increasing temperature difference between the ocean and

[1]Department of Environment and Geography, Center for Earth Observation Science, University of Manitoba, Winnipeg, Manitoba, Canada.

0148-0227/09/2008JC005127$09.00

atmosphere, and when thin first-year ice can easily be fractured by strong winds associated with cyclones. Flux-driven intensification of cyclones may increase if sea ice concentration and extent continues to decline.

[5] Arctic cyclone activity peaks during the summer and is at a minimum during the winter and spring when anticyclonic conditions dominate [*Serreze and Barry*, 1988; *Serreze et al.*, 1993; *McCabe et al.*, 2001]. Cyclonic activity in the Arctic is twice that of anticyclonic activity during the summer months [*Keegan*, 1958; *Serreze*, 1995; *Zhang et al.*, 2004]. Summer cyclones and anticyclones exhibit little regional variability in mean central pressure and are typically 5–10 mb weaker than their winter counterparts [*Serreze et al.*, 1993]. Since the 1960s there has been an increase in the frequency and intensity of cyclones during the winter, spring and autumn. This has been linked to a shift in the average SLP pattern over the Arctic basin, which is attributed to the Arctic Oscillation (AO) [*Thompson and Wallace*, 1998] and Northern Atlantic Oscillation (NAO) [*Serreze*, 1995; *Serreze et al.*, 2000; *Zhang et al.*, 2004]. The negative phase of the AO is characterized by positive SLP anomalies over the Arctic basin and low SLP anomalies at midlatitudes, whereas the positive phase is characterized by a negative SLP anomalies over the Arctic basin, and positive SLP anomalies at midlatitudes. *McCabe et al.* [2001] also suggests that cyclone frequencies oscillate with the state of the AO.

[6] There is considerable interannual variability in cyclone tracks, especially over the Canada basin [*Serreze and Barry*, 1988]. Mean cyclone tracks from 1979 to 1989 show that winter cyclones most frequently enter the Arctic from the Barents and Norwegian seas [*Serreze et al.*, 1993]. Cyclones can also enter from the Pacific Ocean, however, they fill rapidly over Alaska, and those that do reach the Arctic Ocean are much less intense [*Keegan*, 1958]. Recent studies of cyclone variability in the Arctic from 1949 to 2002 [*Sorteberg and Walsh*, 2008] have shown that cyclones generated along the coast of Alaska travel into the East Siberian Sea via the Beaufort Sea during the winter, while during the summer a convergence of cyclones is observed in keeping with earlier studies by *Serreze and Barry* [1988]. This demonstrates the establishment of a minimum in SLP and accompanying BG reversals during summer. Summer Arctic cyclones can also form within the Arctic basin, primarily over Siberia and the Canadian Archipelago. A summer cyclone maximum over the Arctic basin represents a significant area of cyclolysis resulting from the movement and subsequent decay of cyclones into the region [*Serreze*, 1995].

[7] In this study, we examine the relationship between atmospheric circulation and the surface environment in the Southern Beaufort Sea Region (SBSR) by constructing a synoptic climatology consisting of a finite number of atmospheric circulation types [*Yarnal*, 1993; *Barry and Parry*, 2001]. In particular, we propose to develop an understanding of the synoptic weather patterns that precede reversals of the BG. The value of this approach lies in its ability to provide an interpretation of spatial variability in SLP. In this way, large amounts of data can be grouped into manageable categories from which broad conclusions can be made which may account for variability in the BG. This study will focus upon the circulation characteristics of the synoptic weather patterns, and investigate how late spring and summer synoptic weather patterns are linked to BG reversal events. More specifically we address the following research questions: (1) What are the statistically separable types of synoptic-scale sea level pressure patterns over the period 1979–2006 in the SBSR (synoptic climatology)? (2) How do these synoptic types vary temporally (synoptic type variability)? (3) Is there a statistical relationship between the synoptic climatology of the SBSR and the Arctic Oscillation (synoptic types and the AO)? (4) Is there a statistically significant relationship between synoptic types and reversals of the BG (synoptic types and BG reversals)? (5) Is there statistically significant seasonal variability in how BG vorticity responds to the synoptic types (within-type variability of BG vorticity)?

2. Methods

[8] Data encompassing the period 1979–2006 are used in this study. Daily gridded mean sea level pressure data (MSLP) were retrieved from archives maintained by the NOAA-CIRES Climate Diagnostics Centre (CDC) which originate from the National Center for Environmental Prediction (NCEP) Reanalysis I Project [*Kalnay et al.*, 1996]. The spatial resolution of these data is a $2.5^\circ \times 2.5^\circ$ (latitude and longitude) grid, encompassing the Beaufort and Chukchi Sea regions. The boundaries for the synoptic typing exercise (Figure 1) were 55°N, 175°W to 85°N, 120°W, and were selected to capture the Aleutian low and synoptic-scale meteorological features originating over Eurasia and the North Pacific as these may influence the circulation of the BG. This area also includes the Canadian-led Canadian Arctic Shelf Exchange Study (CASES), ArcticNet, and most recent International Polar Year Circumpolar Flaw Lead (IPY-CFL) study regions. Monthly AO climate index data were retrieved from the Department of Atmospheric Science, Colorado State University [*Thompson and Wallace*, 2000].

[9] Sea ice motion data were obtained from the National Snow and Ice Data Center (NSIDC). (There are missing data in 2004, weeks 46–52.) Weekly averages were calculated from a combination of data from the Special Sensor Microwave/Imager (SSM/I), Scanning Multichannel Microwave Radiometer (SMMR), Advanced Very High Resolution Radiometer (AVHRR), and the International Arctic Buoy Program (IABP) buoy data following *Fowler* [2003]. Weekly averages were calculated and then used to compute average weekly vorticity values using finite differencing [see *Lukovich and Barber*, 2006]. The vorticity values are then spatially averaged so as to provide an average measure of rotation within the BG. The spatial extent of the sea ice vorticity calculation is from 125°W to 165°W longitude and 70°N to 80°N latitude (Figure 1) to include the Beaufort Gyre and in keeping with previous studies of temporal BG variability [*Lukovich and Barber*, 2006], and is situated within the limits of the synoptic weather typing exercise. This area is smaller than that used for the synoptic typing exercise so that atmospheric circulation characteristics immediately surrounding the ice vorticity area are considered.

[10] Synoptic-scale atmospheric circulation patterns, hereafter termed 'synoptic types', are classified from daily MSLP data, and then related to sea ice vorticity within the SBSR. The synoptic types are derived using Synoptic Typer 2.2, an application developed by the Australian Bureau of Meteorology [*Dahni*, 2004; also R. R. Dahni and E. E. Ebert, Automated objective synoptic typing to characterize

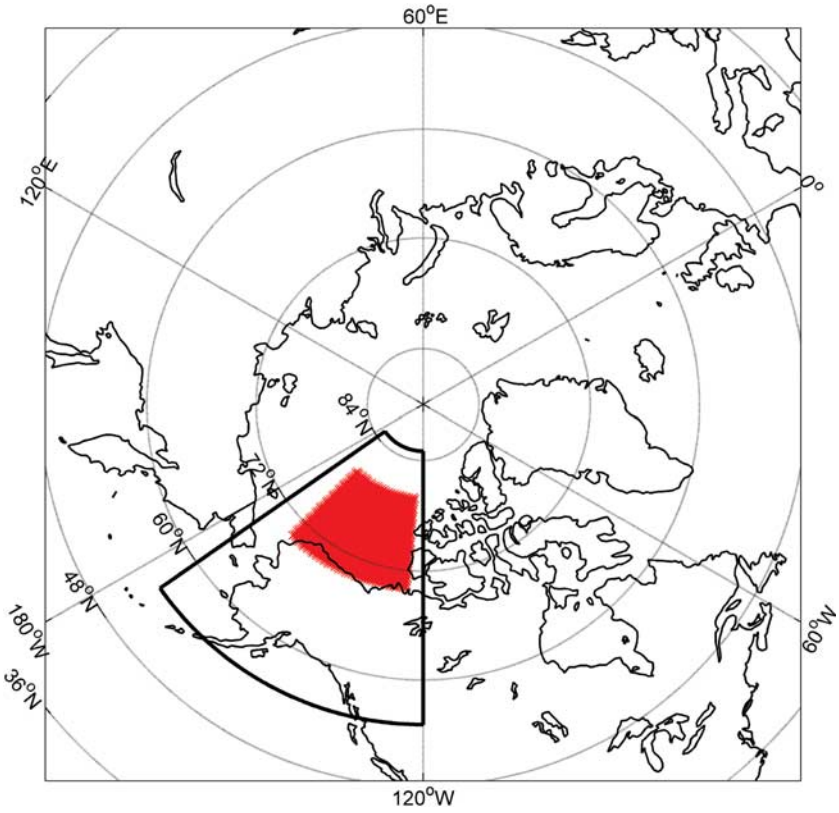

Figure 1. Synoptic typing boundaries (solid line) and sea ice vorticity study area (red).

errors in NWP model QPFs J31–J34, paper presented at 12th Conference of Numerical Weather Prediction, American Meteorological Society, Phoenix, Arizona, 11–16 January 1998]. Synoptic Typer 2.2 applies a commonly used pattern recognition scheme comprising of principal components analysis (PCA) and a subsequent k-means cluster analysis. The user interface of the program allows the researcher to specify temporal and geographical parameters, and more importantly, permits the researcher to easily compare output from schemes using different principal component score and cluster counts.

[11] Daily grids of MSLP data from 1979 to 2006 (9862 days) were processed using Synoptic Typer 2.2. The grids were not standardized (the seasonal effects are retained) because one purpose of the study, among others, is to contrast circulation type characteristics by season. The typing algorithm determines the eigenvalues for the daily MSLP grids from the correlation matrix with no rotation applied. The first six eigenvectors explain 89% of the variability and were retained (Figure 2a). K-means cluster analyses were then performed on the component scores of the retained eigenvectors for 9 to 16 clusters. Cluster distance is the dimensionless difference between a sample (daily calculated component scores) and a cluster centroid. The sample is then assigned to the cluster for which the shortest distance to the cluster centroid is calculated. The mean of the cluster distances within each type represents the cluster homogeneity. Possible cluster-count selections of 10, 12, and 15 are determined by the presence of inflection points in the cluster distance curve (Figure 2b). The cluster distance decreases (increases) as greater (smaller) cluster counts are employed and provides a measure of how closely the actual circulation for each day matches its assigned synoptic type (Table 1). For our study, a 12-cluster solution was chosen as the optimal number on the basis of the inflection point for average cluster homogeneity and the representation of the major synoptic circulation situations in the region.

[12] The output from the clustering algorithm identifies a specific synoptic type for each day of the study period (Figure 3). The representative mean circulation pattern can be visualized with MSLP composites that are created by averaging the gridded MSLP data of all days within each synoptic type. Mean frequency, duration and transition statistics are calculated for the synoptic types, and provide insight into the composition of the synoptic weather patterns of the SBSR (Table 2). Mean monthly occurrence frequencies are then used to show the cumulative frequencies of the types as they occur throughout the annual cycle (Figure 4a).

[13] Given that our interest lies in the summer cyclone season, owing to a predominance of cyclone activity in the Arctic during summer months, we investigate the nature of summer atmospheric circulation patterns upon the circulation within the BG. In addition, we extend the summer into late spring by including the month of May for a ''spring-summer'' season composed of May, June, July, August, September, and October (MJJASO). By including May, our analysis will include any preconditioning within the Beaufort Sea ice gyre that may have arisen from late spring atmospheric circulation patterns. September and October are included to capture the minimum annual sea ice extent, and the associated increase in sea ice mobility.

[14] The average annual synoptic type percent occurrence frequencies are contrasted against those calculated within

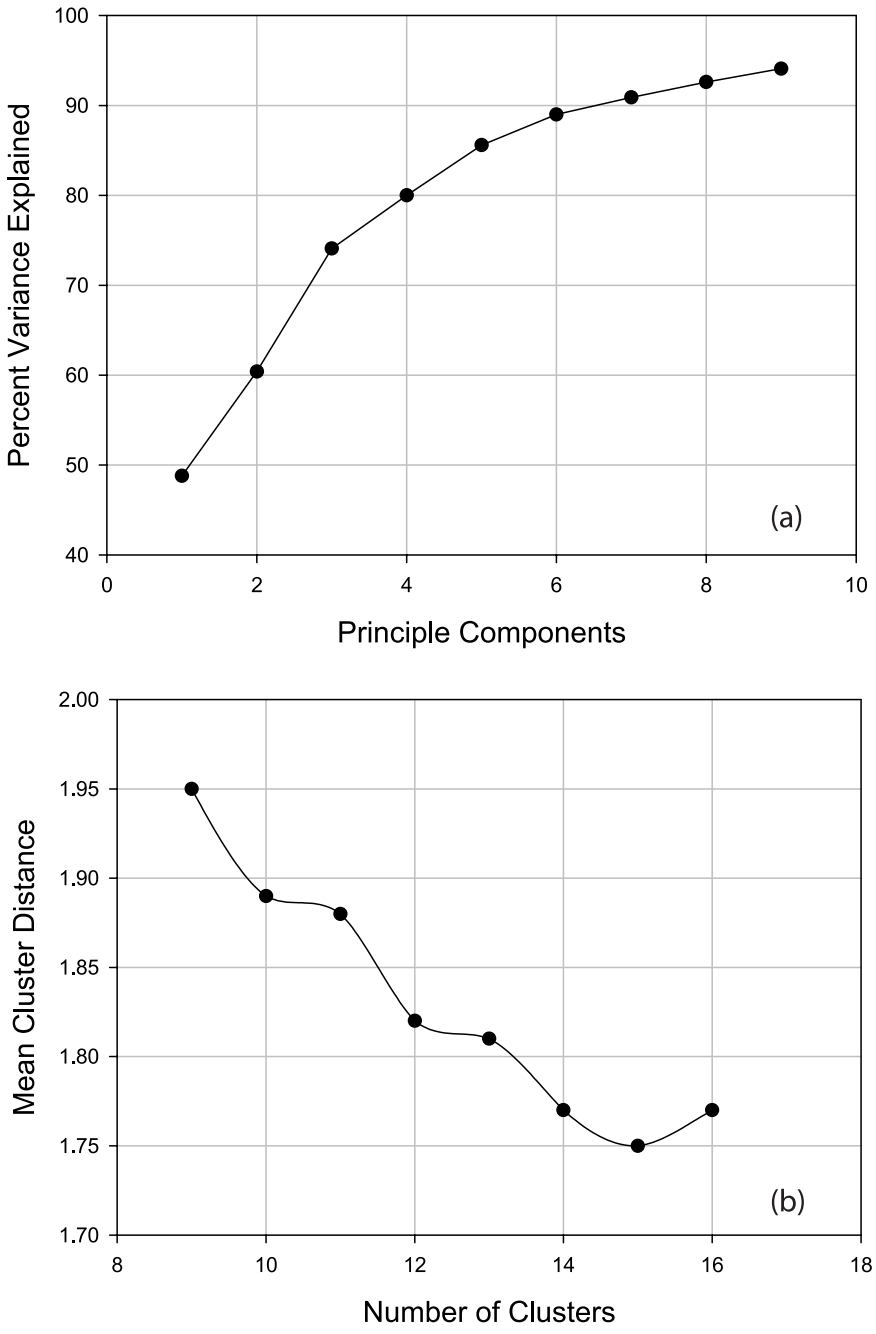

Figure 2. (a) Cumulative variance explained by each principle component and (b) average cluster distance, which represents average homogeneity within the clusters.

the MJJASO and November, December, January, February, March, and April (NDJFMA) seasons (Figure 4b). Decadal large-scale atmospheric circulation variability arising from the AO may affect synoptic type frequencies, and is investigated using chi-square analysis. The synoptic type frequencies are grouped by the corresponding value of the AO index, and are then tested against the mean frequency for each synoptic type for the entire study period. The mean synoptic type frequencies are computed for the positive and negative modes of the AO, and are contrasted against the mean synoptic type frequencies for the study period to create relative frequency anomalies.

[15] An algorithm that combines synoptic type frequency and duration is derived to upscale daily synoptic types to weekly so that we may approximate how each synoptic type influences the circulation of the BG. The data are divided into 7-day periods, effectively creating a weekly interval to which we link atmospheric influences on sea ice motion. If a particular synoptic type occurs or persists for a set threshold within each period, then that synoptic type is assigned to that week to represent the dominant atmospheric circulation influence on sea ice motion. In cases where no particular synoptic type dominates, that week is assigned a null classification. We selected a weekly frequency threshold of three

Table 1. Cluster/Circulation-Type Characteristics for 1979–2006

Synoptic Type	Cluster Homogeneity	Annual Frequency Occurrence of Type (%)	Annual Persistence of Time Same Type Follows (%)	Annual Duration (days)	
				Mean	Max
1	0.61	15.2	56.4	2.3	17
2	1.80	12.4	49.2	2.0	15
3	1.78	11.4	50.1	2.0	11
4	1.74	9.9	48.2	1.9	10
5	1.94	8.8	52.8	2.1	15
6	1.95	7.5	46.0	1.9	9
7	1.91	7.1	38.5	1.6	5
8	1.78	6.4	52.9	2.1	12
9	1.85	6.3	53.2	2.1	10
10	1.89	6.2	41.9	1.7	7
11	1.86	4.8	43.2	1.8	12
12	2.04	4.2	43.2	1.8	12

days, and successfully classify 1185 weeks out of 1456 (81.4%) in the study period. Since 52 weeks comprises of 364 days, 31 December is dropped from each regular year, and 30–31 December are dropped during leap years.

[16] Changes in sea ice motion are known to lag changes in atmospheric forcing at various temporal scales [*Lukovich and Barber*, 2006], and it is therefore prudent to investigate the relationship between the synoptic climatology of the SBSR and BG vorticity at several different temporal scales. We calculate spatially averaged BG vorticity values for running average periods of 2, 4, 6, 8, 10, and 12 weeks. The frequencies of the synoptic types within each of the running average time periods are then correlated to the resulting average BG vorticity. Lag correlations are calculated with BG vorticity lagging the synoptic type frequencies by up to 24-weeks, where zero lag indicates a simultaneous relationship in BG vorticity to a particular synoptic type.

[17] Seasonal within-type variability of BG vorticity is assessed for positive and negative BG vorticity regimes using a Kolmogorov-Smirinov (K-S) test. The K-S test is a nonparametric, distribution-free statistical test that is useful for time series data that may contain serial correlation. The positive (negative) vorticity regimes are first defined as weeks where the average weekly sea ice vorticity is greater than (less than) the threshold of $8.23 \times 10^{-6}\ s^{-2}$. The threshold chosen reflects the first standard deviation of the average annual sea ice vorticity values, and values failing to meet the threshold are dropped. Vorticity generation is defined as a positive or negative change in weekly average sea ice vorticity, from 1 week to the next, and is hereafter referred to as "Δ vorticity." We interpolate daily sea ice vorticity generation values and then link them to the daily synoptic types. We then apply the K-S test to compare the distributions of vorticity generation data between the positive and negative vorticity regimes for within the NDJFMA and MJJASO seasons.

3. Results

3.1. Synoptic Climatology

[18] The synoptic classification yielded 12 synoptic types for the SBSR. The synoptic types are visualized using MSLP composites (Figure 3). The Beaufort high, a prominent semipermanent ridge of high pressure that is situated over the SBSR for much of year, is represented within seven of the twelve synoptic types (types 2, 3, 5, 8, 9, 10, and 12), which exhibit a range of anticyclonic atmospheric circulation patterns. The key difference between these seven synoptic types is the intensity and direction of the geostrophic wind over the SBSR, which is discernable by the varying isobar patterns. The mean center of the Beaufort high varies between synoptic types, appearing over the SBSR in types 2 and 5, Northern Canada in types 8 and 12, over the Canada basin in type 3, and over eastern Siberia in types 6 and 9. In addition, a smaller mean high-pressure system also exists over eastern Siberia in types 6, 7 and 11. Types 2 and 5 both represent a well-developed Beaufort high centered over the SBSR (Figure 3) and, therefore, portray the anticyclone atmospheric circulation regime that persists throughout the cold season. The strong northerly and northwesterly flows of types 2 and 5 over the SBSR likely contribute to the normal anticyclonic rotation of the BG; however type 5 shows a well-developed Aleutian low over the North Pacific which may also impact the circulation of the BG.

[19] Types 10 and 11 show easterly and southeasterly flow patterns over the SBSR, and likely contribute to normal anticyclonic rotation within the BG, and westward ice transport from the SBSR respectively. Type 12 also depicts a deep Aleutian low, but with a southerly flow persisting over the SBSR. This provides strong wind-driven support for anticyclonic rotation in the BG by enhancing the western half of the BG, and thus may increase strain and stress in the sea ice throughout the rest of the SBSR. Prolonged occurrences of type 12 may account for significant moisture and temperature advection into the Arctic basin that may influence sea ice thermodynamics directly through temperature advection, or indirectly through additional precipitation. The weak pressure gradients of the Beaufort high in type 3 show a weakened northeasterly synoptic flow over the SBSR (Figure 3). Type 4 shows a center of mean low pressure situated to the east of the Kamchatka Peninsula, and may represent Pacific storms that track into the Arctic basin. Type 4 also shows a large, weak area of high pressure centered over northern Canada.

[20] The well-developed mean low-pressure features depicted in the synoptic types 1, 6, and 7 represent Arctic cyclones and polar lows. The mean centers of the lows for types 1 and 7 are located over the northern Chukchi Sea, and approximately 200 km west of Ellesmere Island for type 6. The mean pressure gradient of type 1 is weaker than that found in types 6 and 7, which corresponds to weaker cyclones in the summer than during the winter [*Zhang et al.*, 2004]. Types 1 and 7 produce southerly and southwesterly flows, and type 6 yields a northwesterly flow. The origin of cyclones represented by these types is not clearly identifiable from the MSLP composites; however, the location of the mean low pressure in type 6 suggests that it represents cyclones that have tracked into the Arctic basin from the North Atlantic Ocean. Types 1 and 7 may better represent storms tracking in from the North Pacific, or from Eurasia.

[21] There is likely a considerable amount of spatial variability within the synoptic weather classifications, as the illustrations of each synoptic type presented in Figure 3 are merely averages of the gridded daily MSLP within each synoptic type. The spatial variability is lost in the classification and cannot readily be quantified; however, variability in the temporal characteristics of the synoptic types is of great interest.

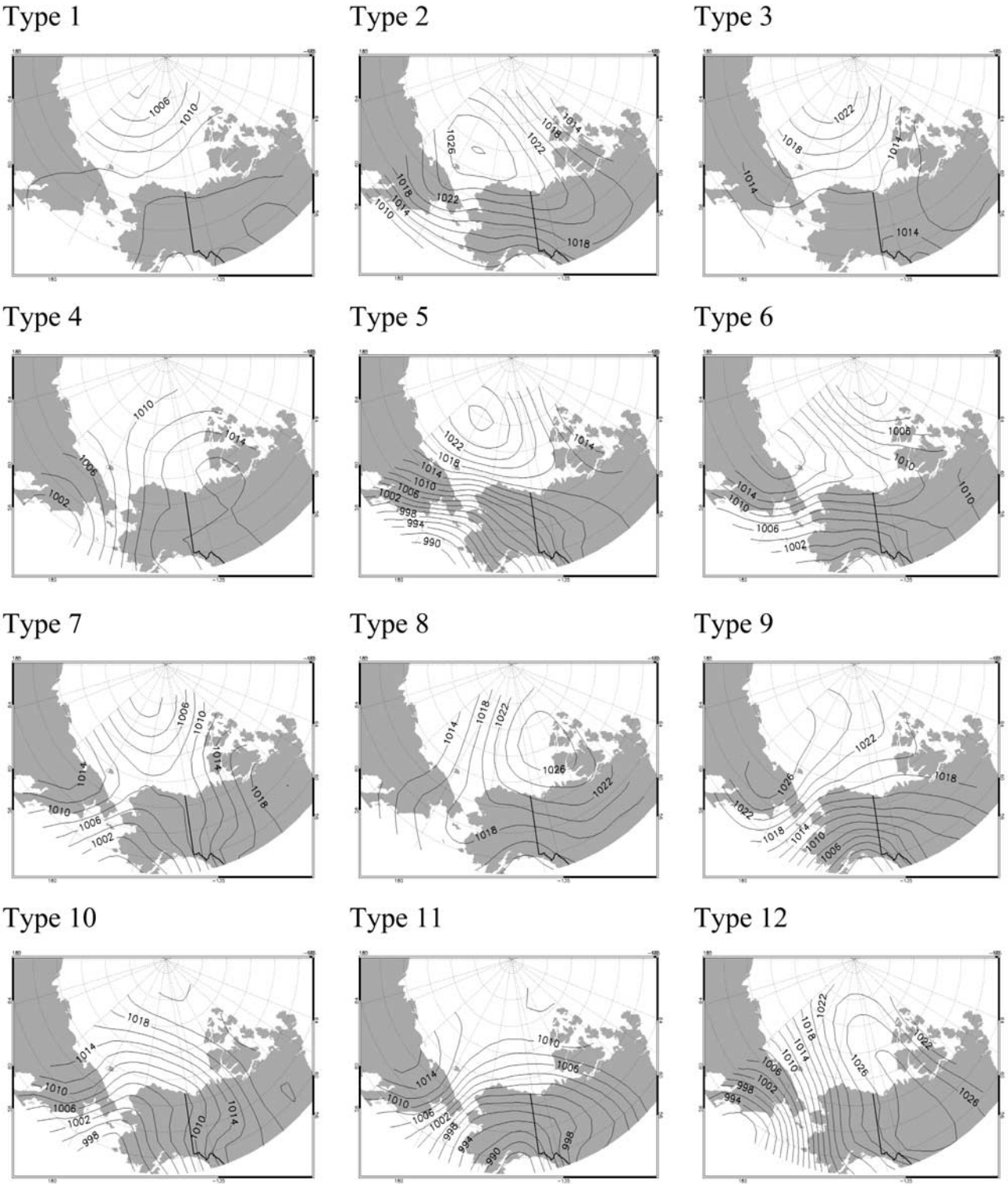

Figure 3. Mean sea level pressure (mb) composites for the 12 synoptic types.

3.2. Temporal Variability of Synoptic Patterns

[22] The synoptic climatology of the SBSR is represented by the pattern in which the synoptic types occur throughout the seasons, and interannual variability is depicted by the frequencies of the synoptic types. The mean frequency, persistence, and duration values are presented in Table 1 for the entire annual cycle and in Table 2 for NDJFMA and MJJASO for each of the synoptic types. The frequencies of some of the synoptic types are highly dependent on season. Some have summer or winter maximum occurrences, and others are year-round types. The seasonal nature of the frequencies of each synoptic type was assessed by calculating occurrence frequency statistics (Figures 4a and 4b).

Table 2. Cluster/Circulation-Type Characteristics for 1979–2006, MJJASO, and NDJFMA Seasons[a]

	Frequency Occurrence of Type (%)		Persistence of Time Same Type Follows (%)		Duration (days)			
					NDJFMA		MJJASO	
Synoptic Type	NDJFMA	MJJASO	NDJFMA	MJJASO	Mean	Max	Mean	Max
1	5.5	24.6	39.6	60.1	1.7	8	2.5	17
2	15.0	9.9	51.5	45.7	2.1	15	1.8	7
3	7.8	15.0	40.9	55.0	1.7	6	2.2	11
4	5.2	14.3	34.1	53.3	1.5	6	2.1	10
5	14.0	3.8	56.0	41.1	2.3	15	1.7	8
6	9.3	5.7	50.8	38.1	2.0	9	1.6	5
7	7.1	7.1	38.5	38.4	1.6	5	1.6	5
8	4.8	7.9	48.8	55.4	1.9	8	2.2	12
9	9.2	3.3	55.8	45.8	2.3	10	1.8	6
10	7.9	4.3	42.6	40.6	1.7	6	1.7	7
11	6.5	2.9	46.9	34.7	1.9	12	1.5	7
12	6.7	1.6	51.7	26.8	2.1	12	1.4	8

[a]MJJASO, May, June, July, August, September, October; NDJFMA, November, December, January, February, March, April.

[23] Type 1 mainly represents summer cyclones, with the highest frequencies occurring during MJJASO (Table 2). Type 6 represents cyclones with a greater mean frequency during NDJFMA. Type 7 is a strong cyclonic type with comparable frequencies for both seasons. Type 2 is anticyclonic type that occurs frequently throughout the year, tending toward higher (lower) frequencies in the winter (summer) season. Types 5, 10, 11, and 12 (anticyclonic types) occur most frequently during the cold season months. Types 3 and 4 (anticyclonic types) occur throughout the year, with a tendency toward higher mean frequencies during MJJASO than during NDJFMA (Table 2). Type 8 (anticyclonic) occurs most frequently from March to July, while type 9 (anticyclonic) occurs more frequently during the NDJFMA season. The results from this investigation suggest that the convergence of cyclones in the Canada Basin in summer noted by *Sorteberg and Walsh* [2008] may be characterized by cyclonic synoptic type 1, whereas cyclones that originated along the Alaska coastline may be associated with wintertime cyclonic types 6 and 7. Values for the mean duration of cyclone types (Table 1) are also consistent with residence times associated with cyclone types entering the Arctic presented by *Sorteberg and Walsh* [2008].

[24] The seasonal persistence and duration of a particular synoptic type is related to its average seasonal frequency, and thus may vary between seasons. Subtracting the persistence values for the NDJFMA from the MJJASO values reveals notable seasonal differences within several synoptic types, where negative (positive) values indicate the type is more persistent in NDJFMA (MJJASO). Type 1 (+20.5%), type 3 (+14.1%), type 4 (+19.2%) and type 8 (+6.6%) are more persistent during MJJASO than during NDJFMA. Type 2 (−5.8%), type 5 (−14.9%), type 6 (−12.7%), type 9 (−10.0%), type 11 (−12.3%), and type 12 (−24.9%) are more persistent during NDJFMA than during MJJASO. Types 7 and 10 show little variability in seasonal persistence.

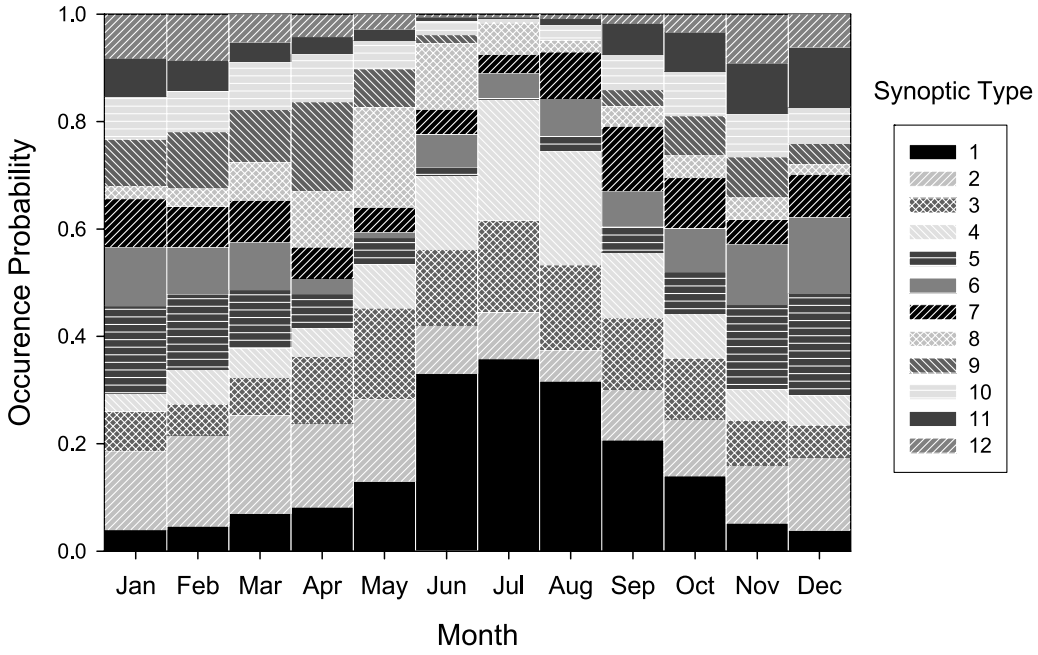

Figure 4a. Cumulative probability distributions of the 12 synoptic types.

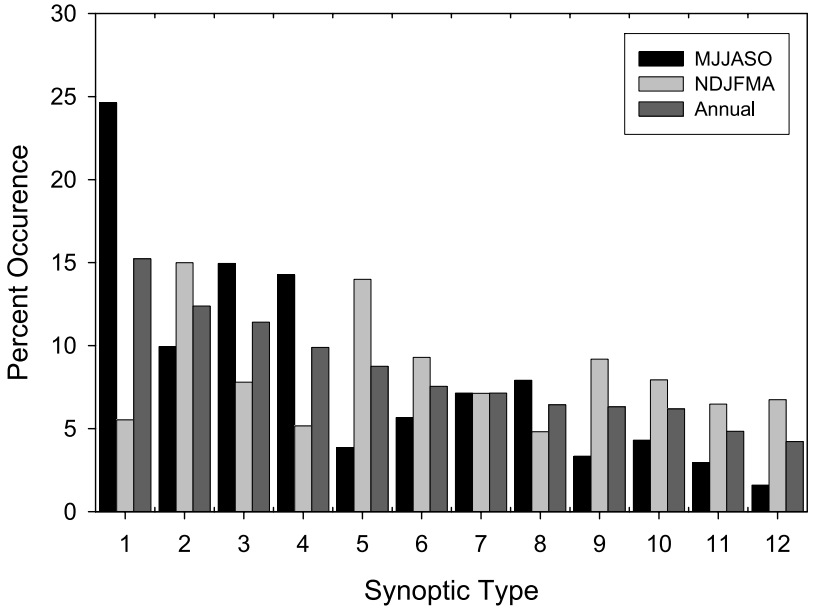

Figure 4b. Synoptic type percent occurrences for within MJJASO, NDJFMA, and the annual cycle.

Comparison of NDJFMA and MJJASO duration statistics reveals that extended durations of types 1, 3, 4, and 8 have occurred during the summer months, with maximum durations of 17, 11, 10, and 12 days respectively. This suggests that higher frequencies of one or more of these types may be at least partly related to reversals of the BG.

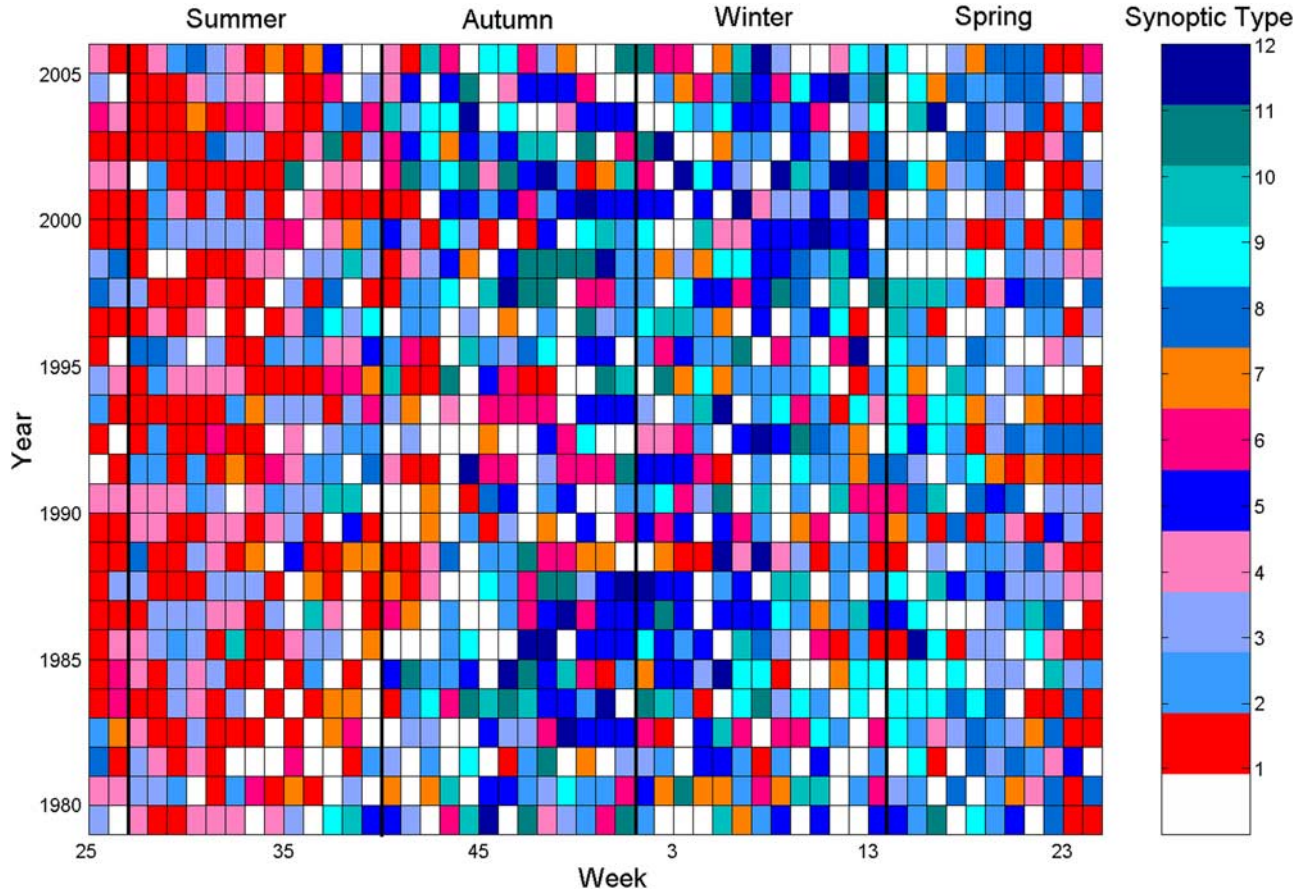

Figure 5. Dominant weekly synoptic types from 1979 to 2006 show weekly types from week 25 to week 24 of the following year. Cyclonic (anticyclonic) types are shown in warm (cool) colors. Weeks with no dominant synoptic type are white.

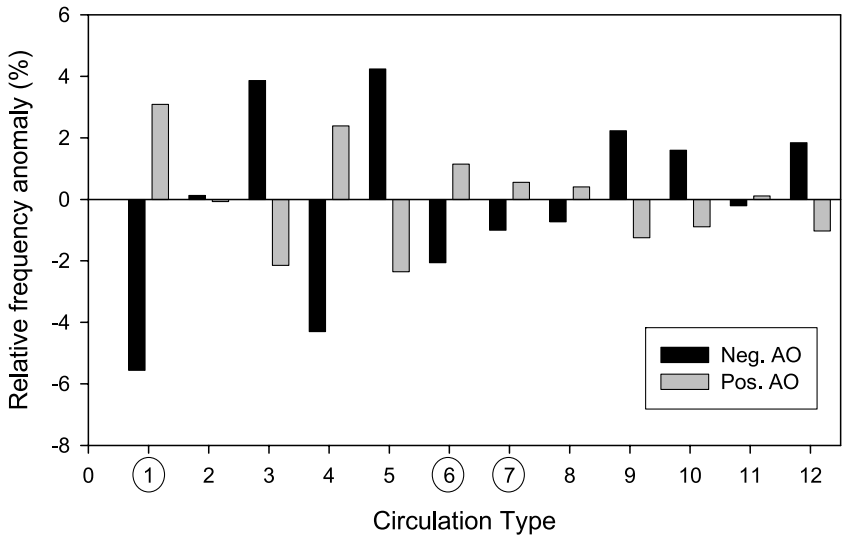

Figure 6. Residuals of the chi-square test of annual synoptic-type frequencies in relation to the Arctic Oscillation with Arctic cyclone types identified by circles.

[25] Weekly synoptic type classifications are created from week 25 of 1979 to week 24 of 2006 (Figure 5). A number of weeks have no dominant synoptic type, and are therefore denoted as 'unclassifiable'.

[26] The week-by-year synoptic patterns for the study period show a general seasonal pattern where types 1, 3, 4, and 8 dominate during the summer season, and types 2, 5, 6, 7, 10, 11, and 12 dominate during the cold season. The occurrence of Arctic cyclone types 1, 6, and 7 during the summer portray the incursion of cyclones into the SBSR. Type 1 is the dominant summer cyclone type, occurring nearly three times as frequently as types 6 and 7 combined (Figure 4b). The frequency of type 7 is somewhat higher in August and September, and thus characterizes some variability in cyclones during the later half of summer. The occasional dominance of high pressure during the summer is represented by types 3 and 4, which both represent high-pressure systems that are centered over different locations. Type 4 also shows a mean center of low pressure situated to the east of the Kamchatcka Peninsula, which likely represents an area of summer cyclogenesis.

[27] The interlaced dominance of types 1, 3, 4, and 8 starts around week 24, and can persist for up to 20 weeks, this represents the synoptic circulation pattern observed over the SBSR when sea ice concentrations are in decline, and increasingly larger areas of open water are present. The combination of pack ice to the north, a marginal ice zone, and areas of open water characteristic of the SBSR may significantly influence baroclinicity during this period and increase the duration and persistence of cyclonic types. A strong summer cyclonic circulation (type 1) can persist for up to several weeks (Figure 5). During the winter, high ice concentrations and a wide sea ice extent help reinforce a cold, stable air mass characteristic of anticyclonic circulation types (types 2, 5, 10–12). Winter Arctic cyclones (types 6 and 7) are less frequent and shorter in duration than summer storms, but are notable features in the winter synoptic climatology of the SBSR. Noteworthy also is the feature where type 1 appears to dominate the summer synoptic circulation pattern more during the latter part of the 20th century and most notably during the early part of the 21st century. In order to understand the mechanisms responsible for decadal-scale variability in synoptic types, connections between large-scale atmospheric circulation patterns characterized by the AO and regional-scale circulation patterns characterized by synoptic types are examined in the next section.

3.3. Synoptic Types and the AO

[28] The AO index is known to be negative for all years from 1979 to 1988, and positive for all years from 1989 to 1995. The AO has been neutral since 1995 [*Comiso*, 2006]. Here the chi-square test shows that interannual variability in the frequencies of the synoptic types is significantly linked to the AO at the 95% level ($p < 0.05$), with the exception of type 2 and 11 (Figure 6). Type 1, a prominent summer Arctic cyclone type, is strongly linked to the AO. An increase (decrease) in frequencies of type 1 corresponds to the positive (negative) phases of the AO. An increase in type 1 may be also be partially attributable to decreasing summer sea ice concentrations and increasing sea ice mobility; however, linking changes in synoptic type frequencies to changes in sea ice concentration is beyond the scope of this paper. The other cyclonic types 6 and 7 also exhibit increased (decreased) relative frequencies when positive (negative) AO conditions dominate. Types 6 and 7 are predominant during the summer and early fall when positive AO conditions prevail. Types 4 and 8 also exhibit increased (decreased) relative frequencies when positive (negative) AO conditions are present. Anticyclonic types 3, 5, 9, 10, and 12 reveal increased (decreased) relative frequencies during negative (positive) AO conditions, just the opposite of the cyclonic types. Noteworthy from this investigation is the existence of a statistical relationship between cyclonic synoptic types and the AO for the SBSR, which reflects the characterization of the positive (negative) AO phase as a period of relatively low (high) Arctic SLP, captured by cyclonic (anticyclonic) synoptic types. Further work is required to investigate how closely the synoptic types are influenced by the AO and

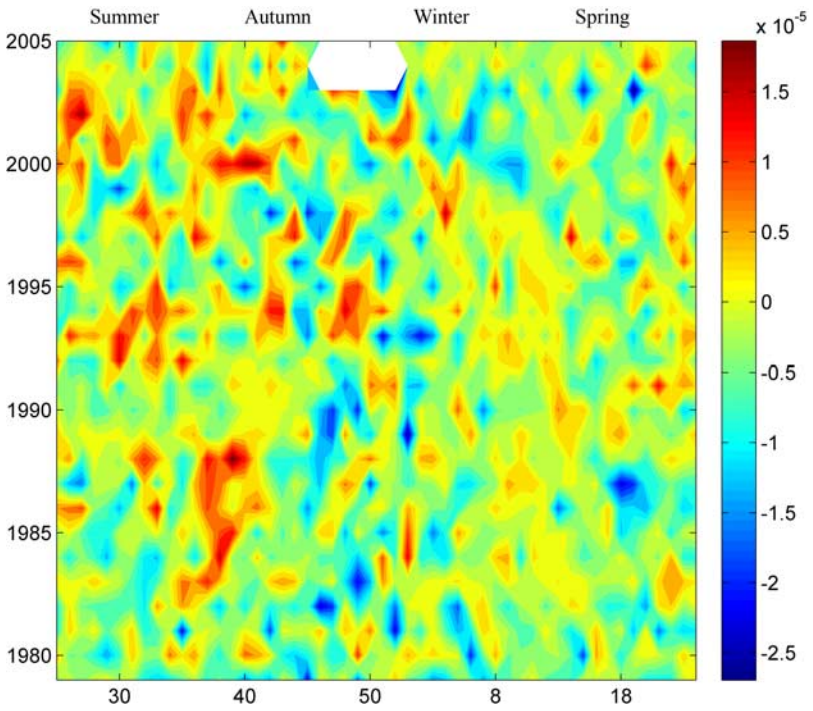

Figure 7. BG average weekly vorticity. Cyclonic (anticyclonic) sea ice motion is indicated in shades of red (blue). Data missing in 2004, weeks 46–52 [after *Lukovich and Barber*, 2006].

whether we could use the AO index as a means of predicting the probability of certain synoptic types, and the response of the sea ice, as a function of season.

3.4. Synoptic Types and BG Reversals

[29] The weekly synoptic types provide a means to link daily synoptic type frequency and persistence to the sea ice spatially averaged weekly vorticity values following *Lukovich and Barber* [2006]. Investigation of mean ice relative vorticity as a function of week and year (Figure 7) highlights reversals in the BG associated with transitions from anticyclonic to cyclonic activity [*Lukovich and Barber*, 2006]. (The white block between autumn and winter for 2003–2005 indicates an absence of data in Figure 7.) Note the predominantly anticyclonic activity throughout the annual cycle, and cyclonic activity during summer and early autumn noted in previous studies [*McLaren et al.*, 1987; *Serreze et al.*, 1989; *LeDrew et al.*, 1991; *Lukovich and Barber*, 2006]. During the 1980s, dominant reversals occurred during summer (weeks 30 to 40), while during the decade of the 90s and into 2000s, reversals occurred over a longer period (weeks 30 to 50), characteristic of the shift from the low-index to the high-index phase in the AO from the 1980s to the 1990s. Following 2000, significant variability in ice relative vorticity is observed throughout the annual cycle, with a return to predominantly anticyclonic activity during winter months. We speculate that this may reflect decreasing sea ice concentrations, and the trend toward the replacement of multiyear ice with first-year ice. Our speculation is that with less ice, and thinner ice, the gyre is becoming more active with detectable reversals occurring throughout a longer period of the annual cycle.

[30] A visual comparison between the weekly synoptic circulation patterns and the weekly sea ice spatially averaged vorticity values in the SBSR demonstrates a relationship between the increased summer frequencies of type 1, and more frequent periods of positive vorticity within the SBSR. Periods of cyclonic activity (positive vorticity) in the BG occur during and following the summer cyclonic atmospheric regime, and conversely, anticyclonic activity (negative vorticity) occurs throughout the rest of the season, corresponding to the persistence of anticyclonic atmospheric synoptic types such as types 2 and 5.

[31] A lag correlation analysis is used to examine connections between synoptic type frequencies and spatially averaged BG sea ice vorticity that have been smoothed with 2-, 4-, 6-, 8-, 10-, and 12-week running means. Lag correlations for 1-week running means were not calculated owing to insufficient daily synoptic type frequencies at that time scale. Lag correlations for 2- and 4-week running means yielded noisy nonsignificant correlations, and were dropped. Stronger correlations emerge as the synoptic type frequency counts increase in the larger running average intervals. The larger time intervals also smooth the lag correlation curves and improve the interpretability of the analysis. Significant correlations appear at a 6-week running mean interval, and lag correlations for 8-, 10-, and 12-week running means reveal a pattern of strengthening significant correlations. We present and interpret the 12-week running average interval (Figure 8) as this interval provides an optimal estimate of lagged correlations between synoptic types and ice relative vorticity.

[32] The lag correlations for the 12-week running average periods show several interesting positive and negative correlations for all types at various time lags, significant at the 95% level ($p < 0.05$) (Figure 8). Positive correlations between frequencies associated with cyclonic synoptic types 1, 6, and 7 and ice relative vorticity for time lags ranging from 0 to 18, 0 to 24, and 9 to 26 weeks,

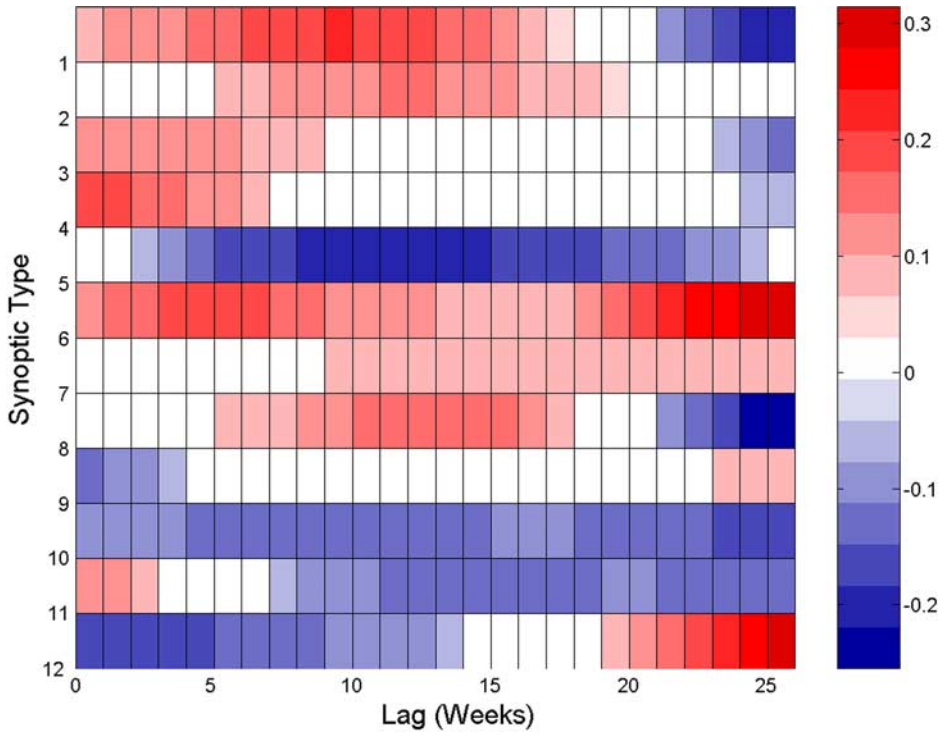

Figure 8. Lag correlations between 12-week running mean synoptic-type frequencies and spatially averaged BG sea ice vorticity data that are significant at the 95% level ($p < 0.05$).

respectively (Figure 8), illustrate correspondence between cyclonic activity in sea ice and atmospheric phenomena. Negative correlations between frequencies associated with anticyclonic synoptic types 5, 9, 10, 11, and 12 for lags of 2–25, 0–4, 0–26, 7–26, and 0–14 weeks, respectively, highlights that an increase in frequency in anticyclonic events results in a decline in ice relative vorticity. Similarity in correlations between types 1 and 3 and ice relative vorticity despite significant differences in circulation patterns for the former may be an artifact of seasonality: the similarity in correlation patterns disappears for data smoothed over shorter (less than 12 week) time scales. Anticyclonic synoptic types 2, 3, 4, and 8 exhibit weakly positive correlations with ice relative vorticity for time lags of 6–18, 0–7, 0–9, and 6–20 weeks, indicating that anticyclonic synoptic types with a displaced Beaufort high or weakened flow over the SBSR will limit the ability of the type to influence ice vorticity.

[33] The apparent contradiction between sea ice relative vorticity and anticyclonic synoptic types may be attributed to regional influence from coastlines in addition to local MSLP patterns, in keeping with previous studies showing negative correlations between ice and atmospheric relative vorticity to 500 mb [*Lukovich and Barber*, 2006], which showed sea ice response to wind stress over the Arctic basin, with regional influence from coastlines and local relative vorticity or, in this instance, local MSLP patterns. The persistence of types 2 and 3 throughout the annual cycle may also result in overlap with residual positive vorticity generated by other cyclone types during summer. Positive (negative) correlations between frequencies of cyclonic types 1 and 6 (anticyclonic types 9, 10, and 12) and ice vorticity at zero time lag also suggest contributions from both cyclonic and anticyclonic synoptic types to reversals in the BG. Moreover, correspondence between types 1 and 6 and ice vorticity at zero time lag indicate contributions from cyclones originating both in the Atlantic and Pacific regions.

3.5. Within-Type Variability of BG Vorticity

[34] Our analysis thus far has focused on the relationship between the frequencies and durations of the synoptic types to BG sea ice vorticity; however, an examination of within-type variability of BG vorticity is also prudent. A synoptic type may generate positive or negative vorticity in the BG, and may exhibit a proclivity toward positive values of Δ vorticity during a particular vorticity regime. The K-S test is employed to compare Δ vorticity distributions within each synoptic type between the positive and negative vorticity regimes. The analysis is conducted for all synoptic types within both of the NDJFMA and MJJASO seasons (Table 3).

[35] The K-S null hypothesis is that within each synoptic type, there is no difference in Δ vorticity distributions between the positive and negative circulation regimes. The K-S statistic D results in larger values representing dissimilarity in the distribution of the two data sets being compared. The calculated value of D is significant at the 95% level ($p < 0.05$) for every synoptic type during both the NDJFMA and MJJASO seasons, and we therefore reject the null hypothesis. These results show that for any given synoptic type, Δ vorticity varies depending on the circulation regime of the BG. Therefore the circulation regime of the BG is a source of within-type variability in atmospheric forcing of the BG.

[36] Another source of within-type variability is seasonal and is likely due to two factors. First, within-type variability in BG vorticity is greatest during the MJJASO season (although D values appear similar for MJJASO and

Table 3. Kolmogorov *D* and *P* Values From a Kolmogorov-Smirnov Test for Seasonal Variability in Δ Vorticity Distributions Between Positive and Negative BG Vorticity Regimes for All Types[a]

	MJJASO		NDJFMA	
Synoptic Type	*D*	*p*	*D*	*p*
1	0.491	**<0.001**	0.503	**<0.001**
2	0.438	**<0.001**	0.487	**<0.001**
3	0.449	**<0.001**	0.560	**<0.001**
4	0.465	**<0.001**	0.563	**<0.001**
5	0.450	**<0.001**	0.407	**<0.001**
6	0.429	**<0.001**	0.467	**<0.001**
7	0.428	**<0.001**	0.550	**<0.001**
8	0.417	**<0.001**	0.405	**<0.001**
9	0.589	**<0.001**	0.534	**<0.001**
10	0.370	**<0.001**	0.479	**<0.001**
11	0.564	**<0.001**	0.528	**<0.001**
12	0.374	**0.007**	0.511	**<0.001**

[a]Boldface is significant at the 95% level.

NDJFMA in types 9 and 11) when ice concentrations and sea ice extent are in decline, and the mobility of the pack ice is greatest. Second, variability in atmospheric circulation may also play a role. A particular synoptic type may exhibit a greater degree of variability in atmospheric circulation patterns and strength, hence having a highly variable influence on BG vorticity. The dimensionless cluster homogeneity values from the k-means analysis show that every synoptic type contains a degree of variability in circulation pattern and strength. This coupled with increasing areas of open water, and increasingly mobile sea ice during the MJJASO season suggests increased sensitivity in BG vorticity to within-type atmospheric circulation variability during MJJASO than during NDJFMA when sea ice extent is growing.

[37] Within-type variability may also arise from coupling between the sea ice cover and the lower troposphere. For example, a strong temperature gradient arising from the interaction of large areas of open water and the pack ice can increase wind speeds considerably and enhance the circulation strength of a given synoptic type. This would be most common in the late summer and autumn when the cold air mass is developing over the pack ice, but areas of open water remain.

3.6. Conclusions

[38] A synoptic climatology is developed for the SBSR that resulted in twelve different synoptic circulation types (Figure 3). The occurrence, spatial pattern, frequency, persistence, and duration of these types is used to assess the synoptic surface pressure pattern of the SBSR from 1979 to 2006 (Tables 1 and 2). The Beaufort high is depicted by synoptic types 2, 3, 5, 8, 9, 10, and 12 characteristic of anticyclonic atmospheric circulation patterns. Cyclonic circulation patterns are characterized by types 1, 6, and 7.

[39] In consideration of our second research question, synoptic weather patterns (Figure 5) vary seasonally. In particular, types 1, 3, 4, and 8 dominate during MJJASO, and types 2, 5, 6, 9, 10, 11, and 12 dominate during NDJFMA. MJJASO is characterized by persistent episodes of cyclone type 1.

[40] Significant large-scale circulation variability arising from the AO is found to be associated with the mean annual frequencies of all synoptic types, with the exception of type 2 and 11. Types 1, 4, 6, 7, and 8 exhibit increased (decreased) relative frequencies when positive (negative) AO conditions prevail. Types 3, 5, 9, 10, and 12 show increased (decreased) relative frequencies during negative AO conditions. The increase (decrease) in the frequencies of summer cyclone types (1 and 6) during positive (negative) AO conditions is identified as a significant large-scale interannual climatic control on BG circulation.

[41] A comparison of weekly spatially averaged sea ice vorticity (Figure 7) data to derived weekly synoptic circulation types suggests that summer reversals are linked to multiple and/or persistent occurrences of Arctic cyclonic synoptic types (1, 6, and 7). Lag correlation analysis between 12-week running mean spatially averaged sea ice vorticity and synoptic type frequencies reveals significant positive correlations between cyclonic synoptic types 1, 6, and 7 for time lags of 0–18, 0–24, and 9–26 weeks, respectively (Figure 8).

[42] The synoptic types appear to contain strong seasonally driven within-type variability in how they force BG sea ice vorticity. This likely arises from varying sea ice conditions (extent and concentration) between MJJASO and NDJFMA, or seasonal variability in atmospheric circulation strength. We expect current trends in the areal extent and thickness of Arctic sea ice to continue to decline [*Intergovernmental Panel on Climate Change*, 2007]. This will result in a more mobile sea ice regime in the southern Beaufort Sea, and likely increase variability in the response of the BG to seasonal atmospheric circulation conditions. The sea ice gyre vorticity will likely increase in magnitude and reversals will most likely increase concomitantly.

[43] This paper has shed light on the relationship between synoptic SLP patterns and their relationship to the motion of sea ice in the BG. Some logical extensions of this work are to examine whether the statistical relationships observed here (between SLP and ice motion) are also found in high resolution coupled ocean-sea and ice-atmosphere models and to determine whether these can be used to explain rapid annual reduction in sea ice extent. Another avenue is to examine in situ effects of these synoptic types on the surface energy balance of the marginal ice zones, through processes of divergence and convergence, of the local ice field. We would also like to see how well the relationship between synoptic types and the AO can be exploited to predict probabilities of atmospheric circulation types and related sea ice motion.

[44] **Acknowledgments.** This work was funded by the Natural Sciences and Engineering Research Council (NSERC), the International Polar Year (IPY) Federal Program Office, and the Canada Research Chairs (CRC) programs through grants to D.G.B. The National Center for Environmental Prediction (NCEP) provided the reanalysis data, and The National Snow and Ice Data Center (NSIDC) provided the passive microwave sea ice concentration data. Thanks to W. Chan for processing the sea ice vorticity data and to Robert Dahni of the Commonwealth Bureau of Meteorology, Melbourne, for permitting us to use Synoptic Typer 2.2. We would like to acknowledge the efforts of the Associate Editor and two anonymous reviewers for improving this manuscript.

References

Barry, R. G., and J. Maslanik (1989), Arctic sea ice characteristics and associated atmosphere-ice interactions in summer inferred from SMMR data and drifting buoys: 1979–1984, *GeoJournal*, *18*(1), 35–44, doi:10.1007/BF00722384.

Barry, R. G., and A. H. Parry (2001), Synoptic climatology and its applications, edited by R. G. Barry and A. M. Carleton, in *Synoptic and Dynamic Climatology*, pp. 547–603, Routledge, London.

Brúmmer, B., G. Múller, and H. Hoeber (2003), A Fram Strait cyclone: Properties and impact on ice drift as measured by aircraft and buoys, *J. Geophys. Res.*, *108*(D7), 4217, doi:10.1029/2002JD002638.

Comiso, J. C. (2006), Abrupt decline in the Arctic winter sea ice cover, *Geophys. Res. Lett.*, *33*, L18054, doi:10.1029/2006GL027341.

Dahni, R. R. (2004), *Synoptic Typer Reference Manual Version 2.2*, Commonw. Bur. of Meteorol., Melbourne, Victoria, Australia.

Fowler, C. (2003), *Polar pathfinder daily 25 km EASE-grid sea ice motion vectors*, http://nsidc.org/data/nsidc-0116.html, Natl. Snow and Ice Data Cent., Boulder, Colo., (Updated 2007.)

Intergovernmental Panel on Climate Change (2007), Climate Change 2007: The Physical Science Basis: Contribution of Working Group I to the Fourth Assessment Report of the Intergovernmental Panel on Climate Change, edited by S. Solomon et al., Cambridge Univ. Press, New York.

Kalnay, E., et al. (1996), The NCEP/NCAR 40-year reanalysis project, *Bull. Am. Meteorol. Soc.*, *77*, 437–471, doi:10.1175/1520-0477(1996)077<0437:TNYRP>2.0.CO;2.

Keegan, T. J. (1958), Arctic synoptic activity in winter, *J. Meteorol.*, *15*, 513–521.

Kwok, R. (2006), Exchange of sea ice between the Arctic Ocean and the Canadian Arctic Archipelago, *Geophys. Res. Lett.*, *33*, L16501, doi:10.1029/2006GL027094.

LeDrew, E. L., D. Johnson, and J. A. Maslanik (1991), An examination of atmospheric mechanisms that may be responsible for the annual reversal of the Beaufort Sea ice field, *Int. J. Climatol.*, *11*, 841–859.

Lukovich, J. V., and D. G. Barber (2006), Atmospheric controls on sea ice motion in the southern Beaufort Sea, *J. Geophys. Res.*, *111*, D18103, doi:10.1029/2005JD006408.

McCabe, G. J., M. P. Clark, and M. C. Serreze (2001), Trends in northern hemisphere surface cyclone frequency and intensity, *J. Clim.*, *14*, 2763–2768, doi:10.1175/1520-0442(2001)014<2763:TINHSC>2.0.CO;2.

McLaren, A. S., M. C. Serreze, and R. G. Barry (1987), Seasonal variations of sea ice motion in the Canada basin and their implications, *Geophys. Res. Lett.*, *14*, 1123–1126, doi:10.1029/GL014i011p01123.

Proshutinsky, A. Y., and M. A. Johnson (1997), Two circulation regimes of the wind-driven Arctic Ocean, *J. Geophys. Res.*, *102*, 12,493–12,514.

Proshutinsky, A. Y., R. H. Bourke, and F. A. McLaughlin (2002), The role of the BG in Arctic climate variability: Seasonal to decadal climate scales, *Geophys. Res. Lett.*, *29*(23), 2100, doi:10.1029/2002GL015847.

Serreze, M. C. (1995), Climatological aspects of cyclone development and decay in the Arctic, *Atmos. Ocean*, *33*(1), 1–23.

Serreze, M. C., and R. G. Barry (1988), Synoptic activity in the Arctic basin: 1979–85, *J. Clim.*, *1*, 1276–1295, doi:10.1175/1520-0442(1988)001<1276:SAITAB>2.0.CO;2.

Serreze, M. C., R. G. Barry, and A. S. McLaren (1989), Sea ice concentrations in the Canada basin, *J. Geophys. Res.*, *94*, 10,955–10,970, doi:10.1029/JC094iC08p10955.

Serreze, M. C., J. E. Box, R. G. Barry, and J. E. Walsh (1993), Characteristics of Arctic synoptic activity, 1952–1989, *Meteorol. Atmos. Phys.*, *51*, 147–164, doi:10.1007/BF01030491.

Serreze, M. C., J. E. Walsh, F. S. Chapin III, T. Osterkamp, M. Dyurgerov, V. Romanovsky, W. C. Oechel, J. Morison, T. Zhang, and R. G. Barry (2000), Observational evidence of recent change in the northern high-latitude environment, *Clim. Change*, *46*, 159–207, doi:10.1023/A:1005504031923.

Sorteberg, A., and J. E. Walsh (2008), Seasonal cyclone variability at 70N and its impact on moisture transport in the Arctic, *Tellus, Ser. A*, *60*, 570–586.

Thompson, D. W. J., and J. M. Wallace (1998), The Arctic oscillation signature in wintertime geopotential height and temperature fields, *Geophys. Res. Lett.*, *25*, 1297–1300, doi:10.1029/98GL00950.

Thompson, D. W. J., and J. M. Wallace (2000), Annular modes in the extratropical circulation, part I: Month-to-month variability, *J. Clim.*, *13*, 1000–1016, doi:10.1175/1520-0442(2000)013<1000:AMITEC>2.0.CO;2.

Yarnal, B. (1993), *Synoptic Climatology in Environmental Analysis: A Primer*, Belhaven, London.

Yu, Y., G. A. Maykut, and D. A. Rothrock (2004), Changes in the thickness distribution of Arctic sea ice between 1958–1970 and 1993–1997, *J. Geophys. Res.*, *109*, C08004, doi:10.1029/2003JC001982.

Zhang, X., J. E. Walsh, J. Zhang, U. S. Bhatt, and M. Ikeda (2004), Climatology and interannual variability of Arctic cyclone activity, 1948–2002, *J. Clim.*, *17*, 2300–2317, doi:10.1175/1520-0442(2004)017<2300:CAIVOA>2.0.CO;2.

M. G. Asplin, D. G. Barber, and J. V. Lukovich, Department of Environment and Geography, Center for Earth Observation Science, University of Manitoba, Winnipeg, MB R3T 2N2, Canada. (asplinm@cc.umanitoba.ca)